ISSN 1063-7788, Physics of Atomic Nuclei, 2023, Vol. 86, No. 11, pp. 1–5. © Pleiades Publishing, Ltd., 2023.
Russian Text © The Author(s), 00000, published in Yadernaya Fizika i Inzhiniring, 00000, Vol. 00000, No. 00000, pp. 00000–00000.

Peculiarities of Crossing and Raising the Synchrotron Transition Energy

S. Kolokolchikov[a],* and Yu. Senichev[a]

[a] *Institute for Nuclear Research (Russian Academy of Science), Moscow, Russia*

**e-mail: sergey.bell13@gmail.com*

Received June 19, 2023; revised June 19, 2023; accepted July 3, 2023

Abstract—The transition energy crossing requires special attention to preserve the stability of the beam during its acceleration to the energy of the experiment. Possible methods of the transition energy crossing in a synchrotron are considered as a case the NICA accelerator complex located in Dubna, Russia.

Keywords: transition energy, slip-factor, γ-jump, superperiod

DOI: 10.1134/S1063778823110236

INTRODUCTION

This article is devoted to the research of methods of crossing and rising of transition energy in circular accelerator complexes during acceleration from injection to the final experiment energy.

NICA collider complex firstly proposed for experiment of heavy ion collisions at the energy $E_{\text{ion}} \sim 4.5$ GeV and polarized proton experiments at $E_{\text{proton}} \sim 13$ GeV. An important characteristic of the synchrotron, depends only on the magneto-optical structure of the accelerator itself, is Transition Energy. During transition energy passage if no measures are taken, instabilities may develop in the synchrotron and finally lead to the loss of the beam. For collider NICA structure, transition energy $E_{\text{tr}} = 5.7$ GeV ($\gamma_{\text{tr}} = 7.1$); thus there is no additional requirements during acceleration of heavy ions, but for proton acceleration to the experiment energy it is necessary. To avoid this problem applies methods of passage transition energy both crossing and variation of transition energy.

The first is a transition energy crossing method, it used widely in synchrotrons still nowadays. When the particle approaches unstable area the transition energy rapidly changes. To research this process, the dynamics of longitudinal motion should be studied taking into account the second order slip-factor as well as the influence of space charge effect. At the same time, it is necessary to monitor the change of the dynamic aperture in a wide range for the various crossing schemes considered. The crossing itself can be carried out by a rapid change in the gradient of quadrupole lenses located on the arcs of the synchrotron.

The second common method – creation a magneto-optical structure with a deliberately high transition energy value [2, 3], thus, the need to pass the transition energy may disappear, since it will obviously be more than the energy of the experiment. So, all instabilities associated with particle movement near the transition energy do not arise at all. It is even possible to create a structure with a complex value of transition energy, with this approach, there will also be no passage of transition energy. Structures of such types were implemented on Moscow Kaon Factory (Russia) [4], SSC Booster (USA) [5], the neutrino factory in CERN (Switzerland) [6] and implemented in the accelerator complex J-PARC (Japan) [7]. This approach is also used for an antiproton storage ring in FAIR (Germany).

TRANSITION ENERGY

With an increase of the particle's energy in the synchrotron, both a change in the particle's momentum and a change in the trajectory length occur. Accordingly, synchrotron frequency which depend on both of these parameters also changes. In general, when determining, it is necessary to take into account the decomposition by degrees of momentum spread $\delta = dp/p$ [8, 9]:

$$\frac{\Delta f}{f_0} = \eta_0\delta + \eta_1\delta^2 + \cdots; \quad (1)$$

$$\frac{\Delta C}{C_0} = \alpha_0\delta + \alpha_1\delta^2 + \cdots. \quad (2)$$

When particle energy approaching the transition value of energy, the influence of the first term in expression (1, 2) begins to be comparable with the second term. In this case η – slip-factor defines as:

$$\eta = \eta_0 + \eta_1\delta + \cdots. \quad (3)$$

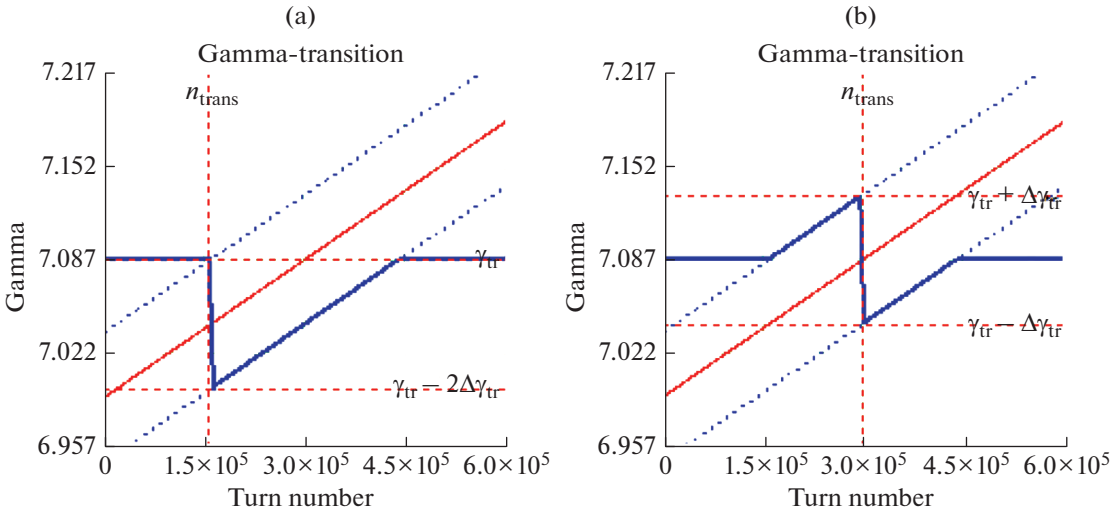

Fig. 1. Schematic diagrams of the transition energy jump. a) jump followed by recovery to the original value; b) preliminary smooth increase of the transition energy, jump and recovery.

For the first two the most significant orders can be getting an expression:

$$\eta_0 = \alpha_0 - \frac{1}{\gamma^2}; \quad (4)$$

$$\eta_1 = \alpha_1 - \frac{\eta_0}{\gamma^2} + \frac{3\beta^2}{2\gamma^2}. \quad (5)$$

PASSING TRANSITION ENERGY USING RAPID JUMP

To minimize beam losses, a rapid change of transition energy is possible. Due to such jump, the time when particles at zero value of slip-factor is significantly reduced. In this case the second order of slip factor $\eta_1\delta$ begins to play a decisive role in the behavior of particles inside RF barrier at separatrix and completely defines the stabile area.

This procedure can be carried out by shifting the betatron frequency, and is associated with a rapid change in gradients in the quadrupole lenses of the arc. The maximum rate of the transition energy change is limited by the quadrupoles parameters and their power systems. For the NICA collider the characteristic values of the increase rate of field gradient in the lens can be given $dG/dt = 14.3\ \frac{\mathrm{T}}{\mathrm{m}\times\mathrm{s}}$, which corresponds to the rise of current rate $dI/dt = 6.4\ \frac{\mathrm{kA}}{\mathrm{s}}$. Installing an additional pulse source with current $\Delta I = 67$ A, leads to fact that the rate of change in the magnitude of the transition energy change is $\dot{\gamma}_{tr} = d\gamma_{tr}/dt = 8.5\ \mathrm{s}^{-1}$, the jump time is $\Delta I/(dI/dt) \cong$ 10 ms. Thus, the total change in transition energy takes on the value $\Delta\gamma_{tr} = 0.09$. [10, 11].

Schematic Jump Diagrams

Figure 1 represent the schematic diagrams of jumps considered for use in the NICA collider. Accelerator operating point for NICA is $\nu_x = 9.44$, $\nu_y = 9.44$. Figure 1a assumes transition energy jump to the value of $\gamma_{tr} - \Delta\gamma_{tr} = 6.997$ with subsequent restoration to the original value. In this case, there is a jump in the betatron frequency to the values $\nu_x = 9.362$, $\nu_y = 9.454$ and it is approaching a third-order resonance, which negatively affects the dynamic aperture and stability of the beam. Figure 1b assumes a preliminary smooth increase up to $\gamma_{tr} + \frac{\Delta\gamma_{tr}}{2} = 7.13$, rapid jump $\gamma_{tr} - \frac{\Delta\gamma_{tr}}{2} = 7.04$ and also restoring to the original value. At the same time, the frequency varies from $\nu_x = 9.4769$, $\nu_y = 9.43$ to $\nu_x = 9.4015$, $\nu_y = 9.447$ and it remains in a stable area. Thus, the second considered jump option is preferable.

The Equations of Longitudinal Motion

The equations of longitudinal motion in coordinates $(\tau, \Delta E)$ is given by Expressions [12, 13]:

$$\frac{d\tau}{dt} = \frac{\eta h}{\beta^2 E_0}\Delta E \quad \text{and} \quad \frac{d\Delta E}{dt} = \frac{Ze}{A}\frac{\omega_0}{2\pi}Ug(\tau), \quad (6)$$

where E_0 – synchronous particle energy, $Ug(\tau)$ – voltage generated by the RF barrier, $\omega_0 = 2\pi/T_0$, h – harmonic number.

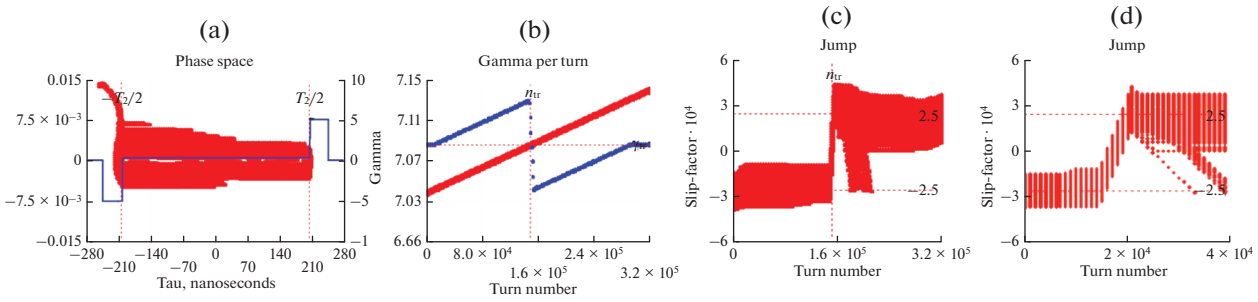

Fig. 2. Passage of the transition energy taking into account the second order of the slip-factor. a) Blurring of the separatrix in the phase plane in the RF-barrier; b) Transition energy jump γ_{tr} (blue dots), γ-particle energy (red dots); c) Slip-factor jump $\eta = \eta_0 + \eta_1\delta$ for various paticles; d) A more detailed scale of the jump.

As can be seen from Equations (6), the voltage generated by the RF barrier is important. In the NICA collider, the RF-1 system is used to retain, accumulate and accelerate particles to the experimental energy in the collider rings. 2 rectangular pulses with opposite signs of the amplitude of each barrier are generated $V_{bb} = \pm 5$ kV. The time duration of a single pulse can vary from $T_{bb} = 10$ to 80 ns. The accumulated particles enclosed between 2 pulses will be inductively accelerated by a constant potential $V_{acc} = 300$ V, which is additionally created also by the RF-1 system. The value of the slip-factor changes sign after the passage of the transition energy and it can be seen from Equations (7) that in order to maintain stable motion, a change in polarity is necessary. When the energy approaches the transition value, the RF barriers are turned off, there is a jump of transition energy as shown on Fig. 1, then the RF barriers are turned on with a change in polarity. On the one hand, with a zero value of the slip-factor $\eta = 0$ the system is isochronous and with any momentum spread, and beam does not increase the length. On the other hand, the following order begins to play an essential role $\eta = \eta_1\delta$, which distorts the movement and can lead to an increase in momentum spread. And finally, in the absence of focusing in the longitudinal plane, the space charge can introduce large distortions into the phase portrait of the beam.

Numerical Simulation

For modeling, in Equations (6) it is convenient to switch from the time derivative to the revolution derivative $t = nT_0$: (also note that for protons $Z/A = 1$)

$$\frac{d\tau}{dn} = \eta\frac{T_0 h}{\beta^2 E_0}\Delta E \quad \text{and} \quad \frac{d\Delta E}{dn} = V(\tau). \qquad (7)$$

For considered jump transition energy changes $\Delta\gamma_{tr} = 0.09$, the value of the slip-factor also is undergoing a change $\Delta\eta_{tr} = 5\times10^{-4}$, thereby reaching the minimum value $|\eta_{tr}| = 2.5\times10^{-4}$ before jump occur Fig. 2c shows that there is a jump of the slip-factor at a different times for different particles due to the dependence of the slip-factor on δ, as it can be seen from Equation (3). After jump, particles with negative value of η will not be located in a stable area, since the polarity of the retaining barriers changes and they will tend to leave the separatrix in the phase plane, what can be seen on Figs. 2a, 2c. Also, due to the momentum spread, an asymmetry of the phase portrait is observed relative to the zero value of the momentum spread $\frac{dp}{p}$.

RESONANT MAGNETO-OPTICAL STRUCTURE WITH HIGH TRANSITION ENERGY

This method is distinguished by the need to make a change in the very magneto-optical structure of the synchrotron and is based on the introduction of a special superperiodic modulation of quadrupole lenses gradients on arcs. To do this, it is necessary to consider the expressions of the momentum compaction factor, without taking into account the higher orders of decomposition:

$$\alpha = \frac{1}{\gamma_{tr}} = \frac{1}{C}\int_0^C \frac{D(s)}{\rho(s)}ds. \qquad (8)$$

From the Expression (8) it can be seen that the value of the transition energy depends both on the dispersion function $D(s)$, and on the function of the curvature of the orbit $\rho(s)$. The latter depends on the arrangement of dipole magnets and cannot be changed in the constructed machine. The dispersion function depends on quadrupole lenses and can be changed by introducing superperiodic modulation even in already created synchrotrons [14].

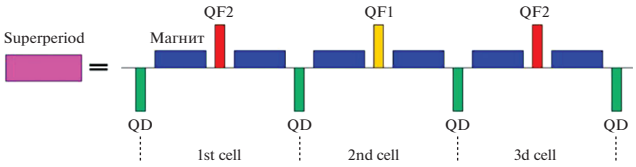

Fig. 3. Schematic diagram of one superperiod consisting of 3 FODO cells. @Key: 1. Superperiod; 2. Magnet; 3. 1st cell; 4. 2nd cell; 5. 3d cell

Introduction of Superperiodic Modulation

One superperiod is defined as a set of FODO cells as, for example, shown on Fig. 3. There are 12 FODO cells in NICA synchrotron arc for which the resonant condition is realized for $S = 4$, $\nu_{x,\mathrm{arc}} = 3$, where S is the number of superperiods on the arc, and 3 FODO cells combined into one superperiod. Thus, due to the tune of betatron oscillations is multiple 2π the arc has the properties of an achromat of the first order.

Modulation of Gradients Depending on the Methods of Dispersion Suppression

To ensure the movement of particles along the equilibrium orbit of the synchrotron on straight sections, it is necessary to ensure zero dispersion. Depending on the method of dispersion suppression at the edges of the arc, the modulations of quadrupole lenses necessary for the realization of the resonant condition also differ. In the case of creating a completely regular arc, this is easily implemented. Figure 4a shows the structure of a regular arc, as can be seen, the dispersion in this case is suppressed automatically due to the choice of the betatron oscillation on the arc multiple of 2π and is an example of a first-order achromat.

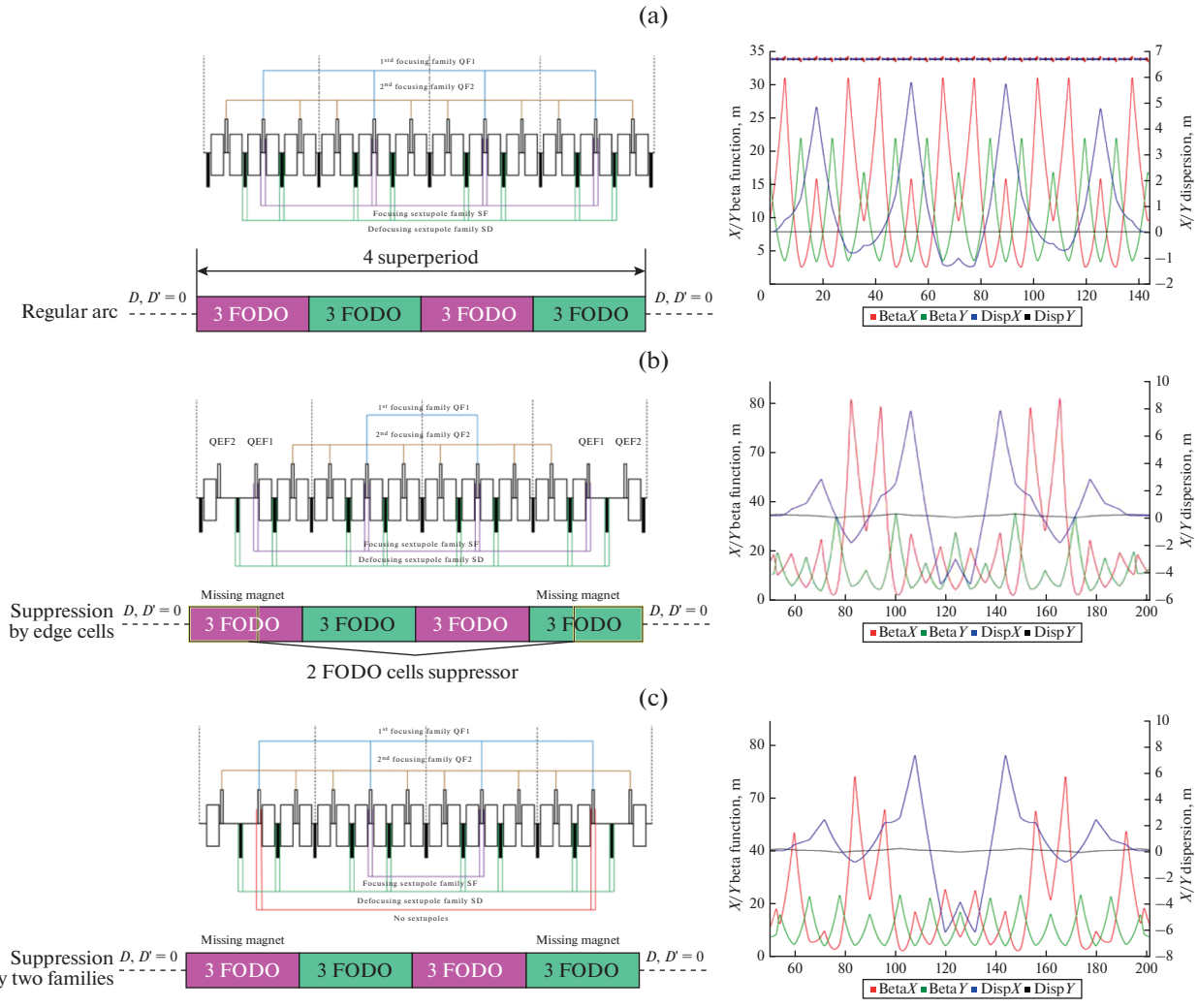

Fig. 4. Schematic diagram of the arrangement of quadrupoles and sextupoles in the collider arc. For a regular structure (a), missing magnet structures with different methods of dispersion suppression: suppression by extreme cells (b), by two families (c). Also on the right are Twiss-functions.

The arcs do not always remain regular, this may be due, for example, to a feature of particle injection in the synchrotron ring, in which the missing magnet method is used when there is no dipole magnet in the FODO cell. In this case, an irregularity occurs due to the non-multiple π of the betatron oscillations, and there is a need for additional suppression of dispersion after the arc. In this regard, it is necessary to consider different methods of dispersion suppression, which also affect the modulation of gradients of quadrupole lenses:

1) ***Suppression by edge cells***. Two FODO cells of edge superperiods is differ by missing magnet, now they contain QFE1 and QFE2 quadrupoles with gradients differ from main arc quadrupoles and is chosen to suppress dispersion. The schematic diagram is shown in Fig. 4 (b).

2) ***Suppression by two families of quadrupoles***. Only 2 families of quadrupole lenses are used for the entire length of the arch. In comparison with option 1), in this case deeper modulation is necessary, but such a scheme does not require the installation of separate batteries Fig. 4c.

CONCLUSION

In this paper, the methods of the transition energy passage that have developed and are used in accelerator technology and can be used in the design of a synchrotron are considered. The problem of the transition energy is associated with those instabilities that, due to various effects, can lead to the loss of the beam. Method of transition energy crossing using a rapid jump, the dynamics of longitudinal motion is investigated taking into account the second order of the slip-factor. Due to the rapid jump of transition energy, the time at which the particles are near the zero value of the slip-factor is significantly reduced, thereby the beam does not have time to disintegrate due to the momentum spread. The method of the transition energy variation (same the method of creating a resonant magneto-optical structure) consists in deliberately raising the value of the transition energy above the energy of the experiment, or even achieving a complex value. In this case, there is no need to overcome the transition energy at all.

FUNDING

This work was supported by ongoing institutional funding. No additional grants to carry out or direct this particular research were obtained.

CONFLICT OF INTEREST

The authors of this work declare that they have no conflicts of interest.

REFERENCES

1. T. Risselada, Report CERN-94-01 (1994), p. 313.
2. Yu. V. Senichev and A. N. Chechenin, J. Exp. Theor. Phys. **105**, 1141 (2007). https://doi.org/10.1134/S1063776107120060
3. Yu. V. Senichev and A. N. Chechenin, J. Exp. Theor. Phys. **105**, 988 (2007). https://doi.org/10.1134/S1063776107110118
4. N. I. Golubeva, A. I. Iliev and Yu. V. Senichev, in *Proceedings of the IEEE Particle Accelerator Conference PAC 1991* (IEEE, 1991).
5. E. D. Courant, A. A. Garren, and U. Wienands, in *Proceedings of the IEEE Particle Accelerator Conference PAC 1991* (IEEE, 1991). https://doi.org/10.1109/PAC.1991.165117
6. B. Autin, R. Cappi, J. Gareyte, R. Garoby, M. Giovannozzi, H. Haseroth, M. Martini, E. Métral, W. Pirkl, H. Schönauer, C. R. Prior, G. H. Rees, I. Hofmann, and Yu. Senichev, in *Proceedings of the 7th European Conference, EPAC 2000, Vienna, Austria, June 26–30, 2000,* Vol. 1–3.
7. Y. Mori, Y. Ishi, M. Muto, H. Nakayama, C. Ohmori, S. Shibuya, T. Tanabe, and M. Tomizawa, in *Proceedings of the European Particle Accelerator Conference EPAC 96.*
8. K. Y. Ng, Fermilab-FN-0713 (2002).
9. J. L. Laclare, in *Proceedings of the CAS CERN Accelerator School: 5th General Accelerator Physics Course*.
10. E. M. Syresin, A. V. Butenko, P. R. Zenkevich, S. D. Kolokolchikov, S. A. Kostromin, I. N. Meshkov, N. V. Mityanina, Y. V. Senichev, A. O. Sidorin, and G. V. Trubnikov, Phys. Part. Nucl. **52**, 997 (2021). https://doi.org/10.1134/S1063779621050051
11. S. Kolokolchikov et al., J. Phys.: Conf. Ser. **2420**, 012001 (2023). https://doi.org/10.1088/1742-6596/2420/1/012001
12. J. Wei and S. Y. Lee, BNL-41667.
13. H. Stockhorst, T. Katayama, and R. Maier, in *Beam Cooling at COSY and HESR Theory and Simulation, Part 1: Theory* (Forschungszentrum, Jülich, 2016), p. 161.
14. S. D. Kolokolchikov and Y. V. Senichev, Phys. At. Nucl. **84**, 1734 (2021).

SPELL OK